ELSEVIER

Catalysis Today 64 (2001) 21–30

CATALYSIS TODAY

www.elsevier.com/locate/cattod

# Partial oxidation of methane
# Effect of reaction parameters and catalyst composition on the thermal profile and heat distribution

F. Basile*, G. Fornasari, F. Trifirò, A. Vaccari

*Dipartimento di Chimica Industriale e dei Materiali, Università degli Studi di Bologna, Viale del Risorgimento 4, 40136 Bologna, Italy*

**Abstract**

The partial oxidation of methane was carried out using new catalysts obtained by calcination and reduction of Mg/Al hydrotalcite-type precursors, containing Rh, Ni or Rh/Ni. The preparation methodology ensured high dispersion of the metal and activity in the partial oxidation of methane. To study the activity, the reaction in autothermal conditions was investigated using IR thermography to monitor the surface temperature. This technique made it possible to monitor the thermal profile of the catalytic bed and the gas/solid heat distribution, following its changes with residence time and reagent concentration. Furthermore, it allowed the diffusion limits to be estimated as a function of the initial ratio between total and partial oxidation of methane. The surface temperature profile was found to be very dependent on the catalyst composition and controlled by the Ni oxidation. For the reforming reactions the outlet composition was compared with the data at equilibrium, calculated at the outlet surface temperature in all reaction conditions. 

*Keywords:* Hydrotalcites; Nickel; Rhodium; Methane partial oxidation; IR thermography; Thermal profile; Heat distribution; Reaction parameters

## 1. Introduction

The use of natural gas as a raw material is a goal of strategic relevance, although there are severe limitations for its exploitation related to the activation of methane [1]. In fact, while the direct processes to $C_2$, formaldehyde or methanol are not attractive due to the low yield values so far obtained, the indirect processes to syngas are still expensive and do not allow intensive exploitation of methane [2,3]. Both academic and industrial researchers have focused much attention on the catalytic partial oxidation of methane as an interesting process to convert methane to liquid products. Although the reaction has been known since Prettre et al. [4] reported the activity of a Ni-based catalyst, enhanced interest in the partial oxidation of methane has resulted from the discovery that high methane conversion and syngas selectivity is possible at low residence times [5–8]. A wide literature reports many active catalysts among which it is difficult to work out the differences [5,8,9]. Furthermore, many aspects of this process are not fully clear, since the large amount of heat produced does not allow a reliable determination of the reaction parameters [7–11].

The reaction temperature has been usually measured by a thermocouple, i.e. determining only the gas phase temperature, or sometimes, by an optic pyrometer which gives an indication of the temperature of the solid [12]. The uncertainty in the determination of the catalyst surface temperature makes it difficult to evaluate the catalytic activity and the role of the

* Corresponding author. Fax: +390-5-120-93680.
*E-mail address:* basile@ms.fci.unibo.it (F. Basile).

0920-5861/01/$ – see front matter 
PII: S0920-5861(00)00505-8

different parameters as well as to understand the reaction mechanism [7,10–12].

The aim of this work was to identify the role of the reaction parameters and evaluate the effects of the catalyst composition at atmospheric pressure and with low dilution of the reaction gas mixture by providing a reliable surface temperature measurement. Furthermore, the role of the reaction parameters and catalyst composition in the control of the surface temperature and thermal profile was evaluated, considering that these aspects are fundamental to control the catalytic performance and the application of the industrial process [13]. In fact, the high pressures of the industrial processes without high temperature control can give rise to the light-off of homogeneous reactions, which can lead to total combustion and flash back of the reaction mixture [13].

The reaction was carried out using new catalysts produced from hydrotalcite-type (HT) precursors [14,15], which after calcination and successive reduction gave rise to small metal particles, well-dispersed inside an inert Mg/Al matrix [16–18], allowing the catalysts to be compared without interference due to different phase compositions.

## 2. Experimental

The catalysts (Table 1) were obtained by calcination and reduction of HT precursors with the general formula $[M^{3+}_{x}M^{2+}_{1-x}(OH)_2](CO_3)^{2-}_{(1-x)/2}mH_2O]$, prepared by coprecipitation at constant pH (a solution containing the nitrate salts of the metal ions was added to a solution containing a slight excess of carbonate) [14,15]. The pH was maintained constant by dropwise addition of 1 M NaOH. The precipitates were kept in suspension under stirring at 60°C for 40 min, then filtered and washed with distillated water until a $Na_2O$ content lower than 0.02 wt.% was obtained. The precipitates were dried overnight at 90°C, calcined for 14 h at 900°C and reduced, where not differently indicated, for 7 h at 750°C in an equimolar $H_2/N_2$ feed of 7 l/h. XRD powder analyses were carried out using a Philips PW1050/81 diffractometer, equipped with a graphite monochromator and controlled by a PW1710 unit ($\lambda = 0.15418$ nm). A $2\Theta$ range from 10° to 80° was investigated at a scanning speed of 70°/h.

The surface areas were determined by $N_2$ absorption using a Carlo Erba Sorpty model 1700. The Ni-particle size was determined by XRD using the simplified Debye–Sherrer equation and the most intense diffraction peaks. The metal particles distribution of the Rh-containing catalyst was determined by analysing the images collected with a TOPCON EM002K HRTEM operating at 200 kV and measuring more than 200 Rh particles. The sample was prepared by suspending a small amount of catalyst in methanol and depositing it on a carbon grid.

The catalytic tests were carried out using an oven heated at 750°C and a $CH_4/O_2/He = 2/1/4$ (v/v) gas mixture or operating in autothermal conditions without an external insulation to allow the IR temperature measurement, and feeding one of the two gas mixtures ($CH_4/O_2/He = 2/1/4$ and 2/1/2, v/v). The reaction was ignited by means of a thermal gun Steinel HG 3000 SLE. The quartz reactor (i.d. 6 mm, e.d. 8 mm) was filled with 0.2 g of catalyst in order to have residence times from 7.2 to 24.0 ms. The gas phase temperature was measured by a chromel–alumel thermocouple measuring 0.5 mm and sliding in a quartz wire (i.d. 1 mm, e.d. 2.5 mm) inside the catalytic bed (length 8–9 mm). The size of the catalyst particles ranged from 0.3 to 0.5 mm, thus the Reynold's number calculated for the $CH_4/O_2/He = 2/1/4$ (v/v) mixture at a temperature of 600°C was between 6 and 22 [19]. This range makes it possible in the case of external heat diffusion limitations to use the following formula to calculate the difference between the gas and the surface temperatures:

$$T_{\text{surf}} - T_{\text{gas}} = \left(\frac{\Delta H^0 C^0_{\text{gas}}}{\rho_{\text{gas}} \nu_i C_p}\right)\left(\frac{C_{\text{gas}} - C_{\text{surf}}}{C^0_{\text{gas}}}\right) \qquad (1)$$

where $T_{\text{surf}}$ is the temperature of the catalyst surface (°C), $T_{\text{gas}}$ the temperature of the gas phase (°C), $\Delta H^0$ the enthalpy of the reaction considered (kJ/mol), $C^0_{\text{gas}}$ the initial concentration of the gas phase (mol/l), $C_{\text{gas}}$ the concentration of the gas phase (mol/l), $C_{\text{surf}}$ the concentration on the catalyst surface (mol/l), $\rho_{\text{gas}}$ the gas density (g/l), $\nu_i$ the stoichiometric coefficient for the *i*-species, $C_p$ the mass specific heat (J/°C g).

The reaction products were analysed on-line after water condensation using two gas chromatographs equipped with HWD and Carbosieve SII columns, having He as the carrier gas for the analysis of $CH_4$,

Table 1
Main characteristics of the Rh- and Ni-containing catalysts

| Sample | Composition | Atomic ratio (%) | Dried at 90°C, hydrotalcite-type phase | | Calcined at 900°C for 14 h | | |
|---|---|---|---|---|---|---|---|
| | | | *a* (Å) | *c* (Å) | Surface area ($m^2$/g) | MgO-type phase *a* (Å) | Spinel-type phase *a* (Å) |
| Rh1 | Rh/Mg/Al | 1/71/28 | 3.072 (7) | 23.13 (3) | 97 | 4.222 (5) | 8.102 (3) |
| Ni10 | Ni/Mg/Al | 10/61/29 | 3.042 (7) | 22.85 (7) | 53 | 4.205 (2) | 8.080 (4) |
| RhNi1 | Rh/Ni/Mg/Al | 0.1/6/59/35 | 3.038 (4) | 22.70 (4) | 88 | 4.209 (3) | 8.084 (3) |
| RhNi2 | Rh/Ni/Mg/Al | 0.1/5/66/29 | 3.050 (6) | 22.87 (6) | 90 | 4.215 (3) | 8.088 (3) |
| Mg/Al | Mg/Al | 71/29 | 3.035 (4) | 22.72 (5) | 83 | 4.217 (1) | 8.086 (2) |

$O_2$, CO and $CO_2$ and $N_2$ as carrier gas for the $H_2$ analysis.

The surface temperature was measured with IR thermography equipment (AGEMA) collecting emitted radiation with λ in the 2–5 μm range. The IR camera was equipped with two zooms to improve the spatial resolution on the catalyst surface and a filter for high temperature applications (>500°C), which allows the utilisation of a narrow λ range. The thermal profile along the length of the catalytic bed was obtained from the maximum temperature indicated by horizontal lines drawn on the thermographic images.

## 3. Results and discussion

### *3.1. Characterisation of the catalysts*

The chemical analyses [18] confirm the quantitative precipitation of all the cations, with compositions corresponding to those of the starting solutions (Table 1). The XRD patterns of the dried precipitates show the presence only of an ordered structure with a pattern corresponding to that of an HT phase, with the crystallographic parameters modified by the presence of the transition metal ions. In particular, the *c* parameter of the Rh sample (Rh1) is larger than that of the corresponding Mg/Al one, since the $Rh^{3+}$ ions have a smaller charge density than the $Al^{3+}$ ions. In the case of the bimetallic RhNi HT phases, the *c* parameters decrease with decreasing Mg/Al ratio as a function of the increased charge density in the brucite-type sheets due to a higher amount of $Al^{3+}$ ions.

The samples calcined at 900°C contain MgO- and spinel-type phases, as expected from HT precursors [14,15]. No segregated Rh- or Ni-containing side phases were found confirming that the transition metal ions are homogeneously distributed together with $Mg^{2+}$ and $Al^{3+}$ ions in the above phases. Previous studies have shown that $Ni^{2+}$ ions form a solid solution together with $Mg^{2+}$ ions in a rock salt-type structure [20], while the $Rh^{3+}$ ions are preferentially solved in the spinel-type phase [16–18].

The XRD pattern of the reduced Ni10 shows the presence of metallic $Ni^0$ with a crystal size of 5–6 nm, while Rh1 does not show peaks related to metallic $Rh^0$. In this case, the distribution of the $Rh^0$ crystal size was obtained using HRTEM. The histograms show a maximum for a crystal size of 1 nm with a narrow distribution, evidencing a high dispersion of the $Rh^0$ in the Mg/Al matrix (Fig. 1). Even though the reduction of the bimetallic RhNi samples was carried out for more than 15 h (a previous study [20] showed that the reduction rate of $Ni^{2+}$ ions decreased as their amount in the sample decreased), the XRD patterns indicate two different behaviours as a function of the Mg/Al ratio (Fig. 2). The XRD pattern of RhNi2, with the higher Mg/Al ratio, shows the partial reduction of $Ni^{2+}$ ions,

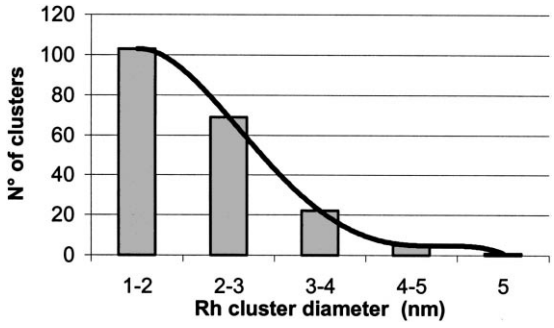


Fig. 1. Size and distribution of the Rh clusters for the reduced Rh1 catalyst.

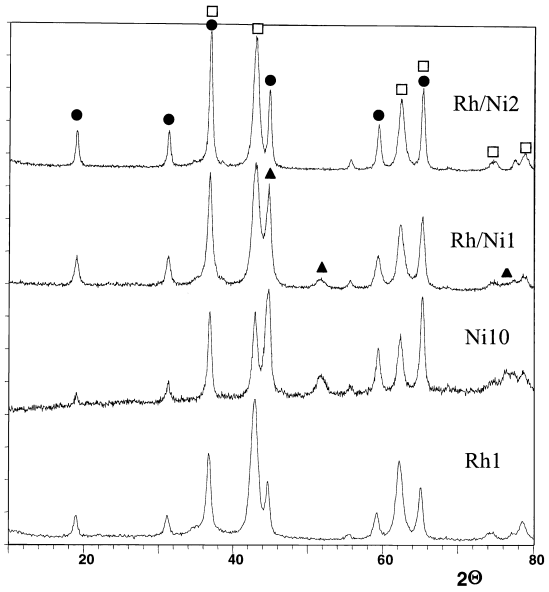


Fig. 2. XRD patterns of the different catalysts after reduction.

while that of RhNi1 shows the complete reduction of the $Ni^{2+}$ ions with an average crystal size slightly smaller than that of Ni10 (4–5 nm). This different behaviour can be explained considering that the dilution of the $Ni^{2+}$ ions in the MgO-type phase is higher in RhNi2 than in RhNi1 (Mg/Ni ratio in the MgO-type phase is about 13 and 10, respectively), thus delaying the reduction of the $Ni^{2+}$ ions.

### 3.2. Catalytic test with an external heat supply

Both XRD and HRTEM of the reduced samples demonstrated that HT phases are good precursors of well-dispersed Rh- and/or Ni-containing catalysts. Their activity in the partial oxidation of methane was investigated operating at 750°C with an external heat supply, a residence time of 11.5 ms and feeding a $CH_4/O_2/He = 2/1/4$ (v/v) gas mixture. Table 2 shows very high conversions of methane and selectivities in syngas, without significant differences between the catalysts. Only the bimetallic sample RhNi2 shows low methane conversion and syngas selectivity, attributable to its partial reduction. These results can be explained considering that with very active and selective catalysts, the differences can be smoothed by the temperature which moves the reaction towards equilibrium. The only appreciable difference is the maximum in the gas phase temperature measured by the thermocouple, which suggests that the heat distribution and thermal profile may be different in the different catalysts. To confirm this hypothesis and to obtain more information on the reactivity of each catalyst, tests in autothermal conditions were carried out, monitoring the surface temperature and drawing the thermal profile.

### 3.3. Catalytic tests in autothermal conditions

The tests were carried out in autothermal conditions using IR thermography to determine the surface temperature and the thermal profile of the catalyst. The surface temperature measurement by IR thermography requires preliminary evaluation of two parameters: (i) transmittance through the quartz wall, found to be equal to 0.9, did not change during the catalytic tests since no deposits were observed on the reactor walls, (ii) the emissivity coefficient. The emissivity coefficient is not tabulated for such complex systems, however, its value in the temperature range of the operating conditions ranges between 0.65 and 0.80 and was assumed to be equal to 0.7, considering the contributions of the support and the metal. The difference in temperature profile calculated by changing the emissivity coefficient from 0.65 to 0.80 was less than 35°C.

Table 2
Activity of the investigated catalysts in the tests of methane partial oxidation carried out with an external heat supply ($T_{oven}$ = 750°C, residence time = 11.5 ms, reaction gas mixture $CH_4/O_2/He = 2/1/4$ (v/v), catalyst composition as in Table 1)

| Sample | $T_{out}$ (°C) | $T_{max}$ (°C) | $CH_4$ conversion (%) | $O_2$ conversion (°C) | CO selectivity (%) | $H_2$ selectivity (%) |
|---|---|---|---|---|---|---|
| Rh1 | 904 | 939 | 93 | 100 | 97 | 95 |
| Ni10 | 888 | 901 | 94 | 100 | 94 | 96 |
| RhNi1 | 866 | 950 | 93 | 100 | 98 | 95 |
| RhNi2 | 840 | 870 | 83 | 100 | 89 | 86 |

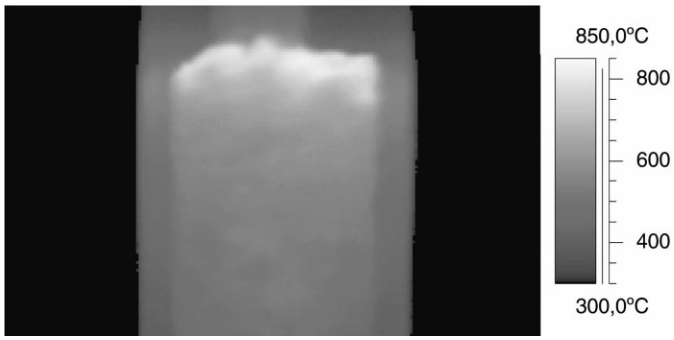


Fig. 3. Thermographic picture of the Rh1 catalyst during the autothermal tests of methane partial oxidation (residence time = 11.5 ms, reaction gas mixture $CH_4/O_2/He = 2/1/4$ (v/v).

The IR thermographic picture of Rh1 and the relative axial profile obtained feeding the $CH_4/O_2/He = 2/1/4$ (v/v) gas mixture at a residence time of 11.5 ms (Figs. 3 and 4) show that the surface temperature in the first part of the catalytic bed increases sharply and reaches the maximum value. On the contrary, the gas phase temperature measured by the thermocouple at the beginning of the catalytic bed was about 220°C lower. This difference in temperature can be explained considering the large amount of heat produced by exothermic reactions, partial and/or total oxidation of methane, and the low efficiency in the heat transfer through the gas–solid interphase. The second part of the catalytic bed is characterized by a decrease in the surface temperature with an almost constant value in the last 4 mm, while the temperature measured by the thermocouple increases to a maximum. In this part of the bed the gas phase temperature is slightly higher than that of the surface, suggesting the occurrence of endothermic reactions. Even if the measurement carried out with the thermocouple can be affected by irradiation of the hot particles around the quartz wire, considering that the ratio between the thermocouple (0.5 mm) and the external dimension of the quartz wire (2.5 mm) is equal to 0.2, only a few percentage of the energy irradiated through the quartz wire reached the thermocouple therefore without a significant effect on the temperature measurement. The radial temperature profile of the same catalyst collected with an angle of 60° confirmed maximum surface temperature at the beginning of the catalytic bed.

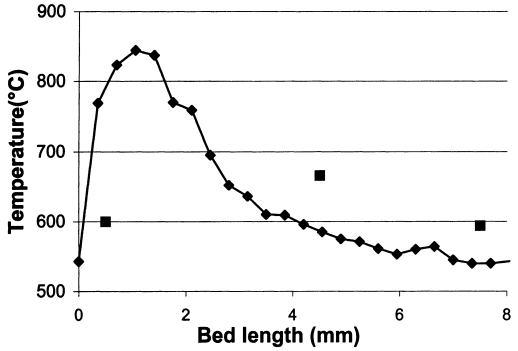


Fig. 4. Surface and gas phase temperature profile of the Rh1 catalyst during the autothermal tests of methane partial oxidation (residence time = 11.5 ms, reaction gas mixture $CH_4/O_2/He = 2/1/4$ (v/v), (◆) surface temperature, (■) gas temperature).

The calculations of the adiabatic temperature and the difference between the gas and the surface temperature at the beginning of the bed allows an evaluation of the relevance of the diffusion limitations as a function of the selectivity in the partial and total oxidation reactions (Table 3). In fact, the calculation of $\Delta H^0$ for the total and partial oxidation reactions makes it possible to evaluate the theoretical difference in temperature between the catalyst surface and the gas phase in the case of total and partial oxidation reactions controlled by heat transport limitations. Fig. 5 reports $(C_{gas} - C_{surf})/C_{gas}$ ($C_{gas} = C^0_{gas}$ at the beginning of the catalytic bed) as a function of the ratio between the selectivity in total or partial methane oxidation, since the amount of each of these reactions in the first part of the bed is not known. Considering the results reported in Table 3 and Fig. 5, it must be noted

Table 3
Fluid-dynamic calculations for the tests with the Rh1 catalyst (residence time 11.5 ms; $CH_4/O_2/He = 2{:}1{:}4$ (v/v))

| | Flow rate ($l\,min^{-1}$) | $\rho_{gas} = 0.1583\,g\,l^{-1}$ |
|---|---|---|
| $CH_4$ | 0.30 | $C_p = 4.284862\,J\,^{\circ}C^{-1}\,g^{-1}$ |
| $O_2$ | 0.15 | $T_{gas} = 600^{\circ}C$ |
| He | 0.60 | $T_{surf} - T_{gas} = 220^{\circ}C$ |
| | Adiabatic $\Delta T$ ($^{\circ}C$)[a] | $\Delta H^0$ at 800°C (kJ) |
| Methane total oxidation | 4723 | −809.4 |
| Methane partial oxidation | 137 | −23.6 |

[a] The adiabatic $\Delta T$ (surface temperature–gas temperature) was calculated considering a total mass transfer limitation ($C_s = 0$).

that the partial oxidation reaction alone would produce a maximum difference in temperature between catalyst surface and gas phase of 137°C with the reaction exclusively under external diffusion control, a difference that would be lower assuming kinetic control. This value is lower than that measured during the tests, thus the occurrence of the more exothermic total oxidation reaction has also to be considered. On the other hand, a large contribution by the total oxidation reaction may be consistent only with very small external diffusion limitations, since the difference between the surface temperature and the gas phase temperature is much less than the value calculated for the total oxidation reaction under diffusion control.

A selectivity in the partial oxidation reaction of the first layer higher than 98% would produce under diffusion control the right temperature difference between catalyst surface and gas phase. Even this value is far from the catalytic data obtained in these conditions (Table 4) and it must also be considered that the first layer has the highest oxygen concentration thus favouring the total oxidation reaction. In conclusion, assuming in the first layer a selectivity in the partial oxidation ≤80% (similar to that observed experimentally), low mass transport limitations ($(C_{gas} - C_{surf})/C_{gas} \leq 0.2$) have to be considered, suggesting a key contribution by surface kinetics and specific catalyst activity.

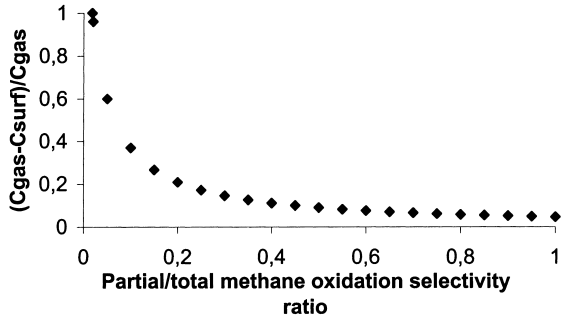


Fig. 5. Contribution of mass transfer limitations as a function of the initial ratio between the selectivities in total and partial oxidation reactions.

The role of the residence time was investigated by increasing the reagent flow rate and monitoring the thermal profile of the catalyst surface. For catalyst Rh1, residence times lower than 11.5 ms gave rise to an increase in the surface temperature mainly at the end of the bed (Fig. 6), and to an enlargement of the hot zone at the beginning of the bed, while the surface temperature at the beginning of the bed did not change. This trend may be explained considering the higher amounts of reagents fed, and consequently, the higher heat production by the exothermic reactions, that supports the higher outlet temperature. On the other hand, the similar values of maximum temperature at the beginning of the bed and the enlargement of the hot zone depend on the rate of the oxidation reactions and evidence that the amount of the heat produced and dispersed on the first catalyst particles remains almost constant with decreasing residence time. This behaviour suggests that at these values of residence time, the influence of the diffusional limitation is almost constant and the amount of the reactant consumed is similar, i.e. that the turnover number is unchanged. The residual oxygen reacts on the second layer of the catalyst with a consequent enlargement of the hot zone and a second temperature maximum. These results are confirmed considering a higher residence time (24.0 ms), for which the trend is opposite and the thickness of the hot zone becomes smaller.

Further information on the role of the residence time may be obtained by comparing the temperatures of the gas phase and catalyst surface at the end of the bed with those of equilibrium for $CO_2$- and steam-reforming reactions, calculated on the basis of the observed gas compositions. At residence time lower than 11.5 ms, both equilibrium reforming temperatures of catalyst Rh1 are very close to that of the catalyst surface, suggesting that the last part

Table 4
Activity of the investigated catalysts in the tests of methane partial oxidation carried out in autothermal conditions (residence time = 11.5 ms, reaction gas mixture $CH_4/O_2/He = 2/1/4$ (v/v), catalyst composition as in Table 1)

| Sample | $T_{inlet}$ (°C) | $T_{outlet}$ (°C) | $T_{max}$ (°C) | $CH_4$ conversion (%) | $O_2$ conversion (%) | CO selectivity (%) | $H_2$ selectivity (%) |
|---|---|---|---|---|---|---|---|
| Rh1 | 600 | 592 | 664 | 66 | 100 | 76 | 86 |
| Ni10 | 581 | 680 | 682 | 72 | 100 | 77 | 92 |
| RhNi1 | 580 | 637 | 655 | 68 | 100 | 72 | 89 |

of the catalytic bed is still active and allows equilibrium to be reached. On the contrary, at 24.0 ms the surface temperature is lower than the equilibrium values, showing that the equilibrium values are reached before the end of the catalytic bed, without the contribution by the last part of the bed.

The thermal profile and the catalytic data obtained at 11.5 ms feeding the $CH_4/O_2/He = 2/1/4$ (v/v) mixture was compared with those of a catalytic test carried out at 16.0 ms by halving He flow rate and keeping constant the flow rates of $CH_4$ and $O_2$ ($CH_4/O_2/He = 2/1/2$ (v/v) of Fig. 6). In this latter case the thermal profile shows a higher peak at the beginning of the bed, with a correspondingly larger difference between surface and gas phase temperature (260°C). This difference can be explained considering the higher reagent concentration and the relative change in the adiabatic temperature, with a value of the temperature difference calculated on this basis of 262°C. The small change in the Reynold's number (11.2 in comparison to 12.0 for the tests with the 2:1:2 and 2:1:4 gas mixtures, respectively) allows the film thickness to be considered unchanged and consequently $((C_{gas} - C_{surf})/C_{gas})$ is also unchanged. These results point out that the concentrations of $CH_4$ and $O_2$ on the surface are different, but these changes do not affect the ratio between the partial and the total oxidation reactions in the first catalyst layer. It is noteworthy that the surface temperature of the two catalysts are almost the same in the further part of the bed, since the total amount of heat produced is the same, and the initial difference in the surface temperature disappears at the outlet. In fact, also in this case, the reaction reaches equilibrium with conversion and selectivity values similar to those obtained in the previous conditions ($CH_4$ conversion 66% , selectivity in CO 76% and selectivity in $H_2$ 87% in comparison to 66%, 76 and 86% with the 2:1:4 gas mixture) (Table 4).

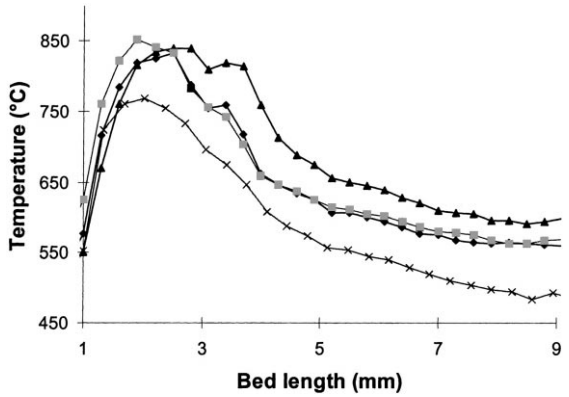


Fig. 6. Surface temperature profile for the Rh1 catalyst, as a function of the residence time and reaction mixture composition ((×) $CH_4/O_2/He = 2{:}1{:}4$ (v/v) 24 ms, (◆) $CH_4/O_2/He = 2{:}1{:}4$ (v/v) 11.5 ms, (▲) $CH_4/O_2/He = 2{:}1{:}4$ (v/v) 7.2 ms, (■) $CH_4/O_2/He = 2:1:2$ (v/v) 16.0 ms).

On the basis of the above findings, the residence time = 11.5 ms was chosen to compare the activity of the Rh1, Ni10 and RhNi1 catalysts in autothermal conditions. Table 4 shows better catalytic performance for the Ni10 catalyst in comparison to the Rh1 catalyst, attributable to a higher outlet surface temperature (compare Figs. 7 and 8).

The temperature of the gas phase measured by the thermocouple is different for the three catalysts (Table 4), suggesting even larger differences in the surface temperature. In fact, the thermal profile of the Ni10 catalyst is very different from that of the Rh1 catalyst, showing a broader peak with a lower maximum surface temperature positioned in the middle of the catalytic bed (Fig. 9). On the contrary, in the second part of the catalytic bed the surface temperature is higher for Ni10 than for Rh1, with a correspondingly higher temperature measured by the thermocouple, due to the broadening of the hot zone which improves the heat transport efficiency from the solid to the gas phase. Furthermore, the difference between gas and

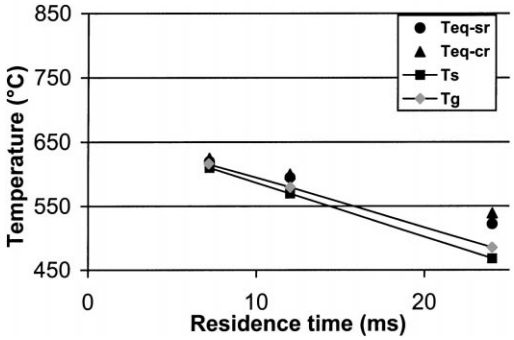


Fig. 7. Comparison as a function of the residence time of the (◆) gas and (■) catalyst surface temperature at the end of the catalytic bed with those of equilibrium for the (▲) $CO_2$- and (●) steam-reforming reactions, calculated on the basis of the gas outlet composition in the tests of methane partial oxidation using the Rh1 catalyst.

surface temperature at the end of the bed is larger for the Ni10 than for the Rh1 due to the occurrence of endothermic reactions in this zone.

Notwithstanding the difference in the thermal profile, also with Ni10 for residence time $\leq 11.5$ ms both the $CO_2$- and steam-reforming reactions are close to the thermodynamic equilibrium calculated on the basis of the outlet surface temperature, even if below the thermodynamic equilibrium calculated on the bases of the gas phase temperature (Fig. 8).

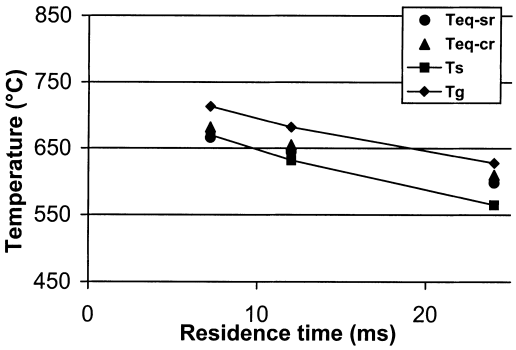


Fig. 8. Comparison as a function of the residence time of the (◆) gas and (■) catalyst surface temperature at the end of the catalytic bed with those of equilibrium for the (▲) $CO_2$- and (●) steam-reforming reactions, calculated on the basis of the gas outlet composition in the tests of methane partial oxidation using the Ni10 catalyst.

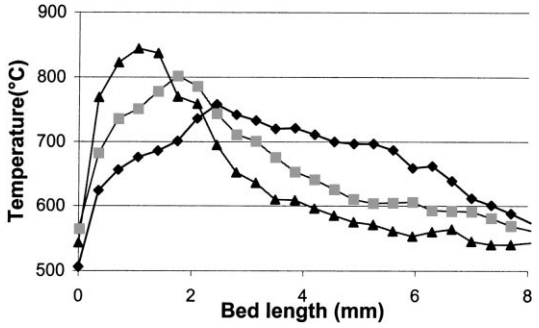


Fig. 9. Surface temperature profile of catalysts (▲) Rh1, (◆) Ni10 and (■) RhNi1 in the tests of methane partial oxidation carried out in autothermal conditions (residence time = 11.5 ms, reaction gas mixture $CH_4/O_2/He = 2/1/4$ (v/v)).

The radial profile of the Ni10 catalyst collected at 60° (Fig. 10) shows that the distribution of the surface temperature at the top of the catalytic bed is not homogeneous; only some particles are active and hot. This behaviour can be explained by a temperature-dependent redox equilibrium. At the beginning of the bed, the $O_2$-rich gas mixture oxidizes the $Ni^0$ to NiO and deactivates the particles, nevertheless with increasing temperature the oxidation power of the gas mixture decreases and the amount of $Ni^0$ is sufficient to light-off the reaction. The amount of $Ni^0$ increases gradually along the bed giving rise to the observed profile. The ignition of the reaction was repeated reaching almost the same steady-state tem-

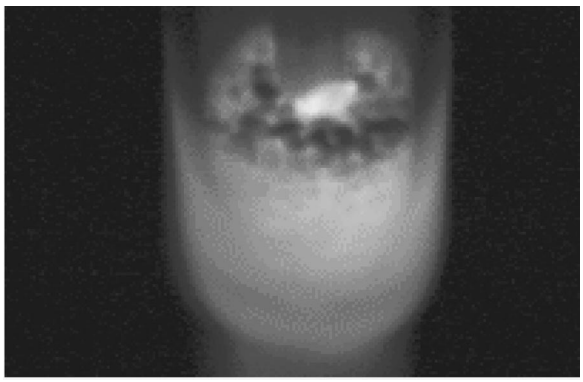

Fig. 10. Radial thermography picture for the Ni10 catalyst during the tests of methane partial oxidation carried out in autothermal conditions (residence time = 11.5 ms, reaction gas mixture $CH_4/O_2/He = 2/1/4$ (v/v)).

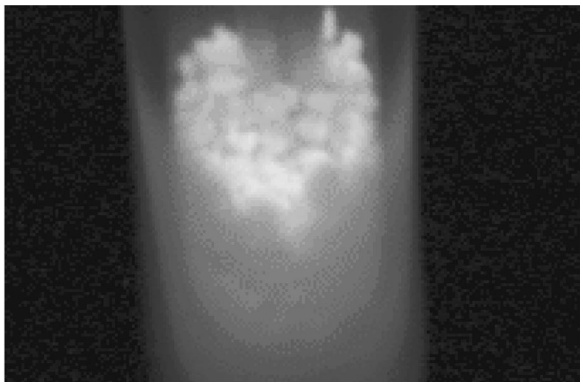

Fig. 11. Radial thermography picture for the Rh/Ni1 catalyst during the tests of methane partial oxidation carried out in autothermal conditions (residence time = 11.5 ms, reaction gas mixture $CH_4/O_2/He = 2/1/4$ (v/v)).

perature profile which therefore has to be considered as determined by catalyst composition and reaction conditions.

The RhNi1 catalyst shows an intermediate thermal profile (Fig. 9) due to the lower formation of NiO at the beginning of the catalytic bed. However, the surface temperature at the beginning of the bed is not very high, as seen from the radial thermal profile, which also shows a homogeneous distribution of the temperature (Fig. 11). With the RhNi1 sample, the whole catalytic bed was black-grey, without detectable zones with different degrees of Ni oxidation. Thus, the presence of Rh increases the surface temperature and consumes the $O_2$ fed at the top of the bed, and consequently prevents the $Ni^0$ reoxidation.

It is noteworthy that the differences among the Rh, Ni and Rh/Ni catalysts are due to a different thermal profile and heat distribution and therefore are more evident on the bases of IR thermography than on the basis of the catalytic data, since in many cases the catalytic data are determined in reference to the outlet surface temperature, which gives wrong indications on the activity and specificity of each catalyst in the partial oxidation reaction.

## 4. Conclusion

HT phases are useful precursors of Ni- and/or Rh-based catalysts. Calcination of these precursors followed by reduction leads to well-dispersed metal particles stabilized in an inert matrix. The reduction conditions to obtain the metallic Ni depend on the ratio between the Ni/Mg in the rock-salt type (Ni/Mg)O phase obtained by calcination and thus by the Mg/Al ratio in the starting precursors.

The catalysts in the tests carried out with an external heat supply all show high methane conversion and syngas selectivity, without significant differences with the exception of the gas phase temperature.

In the tests carried out in autothermal conditions, the Rh1 catalyst showed the presence of the exothermic reactions in the first layers of the catalytic bed, with a strong difference between gas and surface temperature, due to strong exothermic reactions and small mass transport limitations. In these conditions, the surface activity of the catalyst plays a key role in the overall kinetic reaction of the first layer of the catalytic bed. The outlet gas compositions for residence times $\leq$ 11.5 ms could be explained by the thermodynamic equilibria of the $CO_2$- and steam-reforming reactions calculated at the outlet temperature.

A decrease in the residence time changes considerably the temperature of the bed, broadening the initial hot zone and increasing the outlet temperature, with a consequent increase in methane conversion and syngas selectivity. On the contrary, an increase in residence time decreases the outlet temperature, which no longer affects the conversion and selectivity data.

The reagent concentration affects the thermal profile at the beginning of the catalytic bed, although this difference disappears at the outlet, thus without significant effects on the catalytic data. The difference at the beginning of the bed may be explained considering the large amount of heat produced due to the change in the surface concentration without affecting the ratio between the selectivity in the partial and total oxidation reactions.

The different catalysts investigated show the following scale of methane conversion and syngas selectivity: Ni10 > RhNi1 > Rh1 that can be explained on the basis of the different heat distribution and outlet surface temperature, which is maximum for the Ni10 catalyst due to its broader thermal profile related to the partial oxidation of the $Ni^0$ in the first layers of the catalyst. The presence of the Rh in the RhNi1 catalyst prevents the oxidation of the $Ni^0$, suggesting a way to tune the surface thermal profile.

## Acknowledgements

F. Basile thanks Prof. A. Kiennemann (ECPM, LERCSI, Strasbourg) for his helpful assistance and scientific contribution. Financial support from the Ministero per l' Università e la Ricerca Scientifica e Tecnologica (MURST, Rome) is gratefully acknowledged.

## References

[1] M. Colitti, in: A. Parmaliana, D. Sanfilippo, F. Frusteri, A. Vaccari, F. Arena (Eds.), Natural Gas Conversion V, Studies in Surface Science and Catalysis, Vol. 119, Elsevier, Amsterdam, 1998, p. 1.
[2] P. Courty, P. Chaumette, Energy Progress 27 (1987) 1.
[3] A. Solbakken, in: A. Holmen, K.-J. Jens, S. Kolboe (Eds.), Natural Gas Conversion, Studies in Surface Science and Catalysis, Vol. 61, Elsevier, Amsterdam, 1991, p. 225.
[4] M. Prettre, C. Eichner, M. Perrin, Trans. Faraday Soc. 43 (1946) 335.
[5] A.T. Ashcroft, A.K. Cheetham, J.S. Foord, M.L.H. Green, C.P. Gray, A.J. Murrel, P.D.F. Vernon, Nature 344 (1990) 319.
[6] D. Dissanayake, M.P. Rosynek, K.C.C. Kharas, K.J. Lunsford, J. Catal. 132 (1991) 117.
[7] D.A. Hickman, E.A. Haupfear, L.D. Schmidt, Catal. Lett. 17 (1993) 223.
[8] G.A. Foulds, J.A. Lapszewicz, Catalysis, The Royal Society of Chemistry, Cambridge, UK, Vol. 11, 1994 (Chapter 10).
[9] V.R. Chaudhary, A.M. Rajput, V.H. Rane, Catal. Lett. 16 (1992) 269.
[10] K. Walter, O.V. Buyeskaya, D. Wolf, M. Baerns, Catal. Lett. 29 (1994) 261.
[11] E.P.J. Mallens, J.H.B.J. Hoebink, G.B. Marin, Catal. Lett. 167 (1997) 43.
[12] Y. Chang, H. Heineman, Catal. Lett. 21 (1993) 215.
[13] L.D. Schmidt, O. Deutschmann, C.T. Goralsky, in: A. Parmaliana, D. Sanfilippo, F. Frusteri, A. Vaccari, F. Arena (Eds.), Natural Gas Conversion V, Studies in Surface Science and Catalysis, Vol. 119, Elsevier, Amsterdam, 1998, p. 685.
[14] F. Cavani, F. Trifirò, A. Vaccari, Catal. Today 11 (1991) 173.
[15] F. Trifirò, A. Vaccari, in: J.L. Atwood, J.E.D. Davies, D.D. McNicol, F. Vögtle (Eds.), Comprehensive Supramolecular Chemistry, Vol. 7, Pergamon Press, Oxford, 1996, p. 251.
[16] F. Basile, L. Basini, G. Fornasari, M. Gazzano, F. Trifirò, A. Vaccari, J. Chem. Soc., Chem. Commun. (1996) 2435.
[17] F. Basile, L. Basini, G. Fornasari, M. Gazzano, E. Poluzzi, F. Trifirò, A. Vaccari, in: B. Delmon, P.A. Jacobs, R. Maggi, J.A. Martens, P. Grange, G. Poncelet (Eds.), Preparation of Catalyst VII, Studies in Surface Science and Catalysis, Vol. 118, Elsevier, Amsterdam, 1998, p. 31.
[18] F. Basile, G. Fornasari, M. Gazzano, A. Vaccari, Appl. Clay Sci. 16 (2000) 185.
[19] R.H. Perry, C.H. Chilton, Chemical Engineers Handbook, Vth Edition, McGraw-Hill, New York, 1973.
[20] F. Basile, L. Basini, M. D'Amore, G. Fornasari, A. Guarinoni, D. Matteuzzi, G. Del Piero, F. Trifirò, A. Vaccari, J. Catal. 173 (1998) 247.